Evaluation of the Accuracy of Centrifugal Pumps Complete Characteristics and Their Approximation Using Fourier Series

Krzysztof Karaśkiewicz and Jacek Szymczyk*

Instytute of Heat Engineering, Faculty of Power and Aeronautical Engineering, Warsaw University of Technology, Nowowiejska 21/25, 00-665 Warsaw, Poland
E-mail: krzysztof.karaskiewicz@pw.edu.pl; jacek.szymczyk@pw.edu.pl
**Corresponding Author*

Received 28 August 2023; Accepted 18 September 2024

Abstract

The complete characteristics used by commercial codes to simulate failures in pumping systems encountered e.g. in power plants, date back many decades. Since then, pump design methods have changed, resulting in, among others, the increase of their efficiency and the stability of characteristics. There is a need to see how these changes have affected the complete characteristics in a full range of pump operation. In the article, it is shown that the new complete characteristics give different failure simulation results than the old ones. Describing the dynamic pump operation, understood as determining the basic parameters that change at any time, such as: flow, lifting height, driving torque and rotational speed, is very important, especially for large installations whose operation is of key importance. A convenient form for analysing dynamic states are Suter functions based on inverse trigonometric

International Journal of Fluid Power, Vol. 26_1, 25–42.
doi: 10.13052/ijfp1439-9776.2612

functions, because they allow showing all pump operating states using one continuous (other than e.g. spline) function. Therefore, as an approximation of the exact characteristics, Fourier harmonic functions were proposed. The effect of the approximation on the accuracy of the simulation was checked.

Keywords: Rotodynamic pumps, complete pump characteristics, abnormal states of pump operation.

List of basic symbols

h – dimensionless head $h = H/H_n$
q – dimensionless flow rate $q = Q/Q_n$
m – dimensionless torque $m = M/M_n$
α – dimensionless rotational speed $\alpha = n/n_n$
$\psi = \frac{gH}{n^2 d^2}$ head coefficient
$\Phi = \frac{Q}{nd^3}$ flow coefficient
$\pi = \frac{P}{\rho n^3 d^5}$ power coefficient
$n_q = \frac{n\sqrt{Q}}{(H/stage)^{0.75}}$ specific speed
θ – Suter's flow/speed coefficient (4)
WH – Suter's head coefficient (5)
WB – Suter's torque coefficient (6)
u_{WH} – relative uncertainty of extrapolated *WH* (7)
u_{WM} – relative uncertainty of extrapolated *WM* (8)
u_θ – relative uncertainty of extrapolated *WM* (8)
PAT – Pump As Turbine mode
BEP – Best Efficiency Point
Subscripts
n – nominal value for rotational speed and *BEP* for other parameters
Q, *H* and *M*

1 Introduction

Section 1 presents how the description of pump operation has developed over the years in the widest possible range of possible operating states and how the

characteristics of centrifugal pumps can be presented in the simplest possible way.

Over the past half century, blade channel design methods for centrifugal pump impellers have developed significantly through the use of CFD. Blade channel optimization methods such as [1, 2] have begun to be applied, which has led to improvements in pump characteristics. A comparative study by one of the authors at a pump manufacturer's test station using old pumps from half a century ago shows that modern pumps tend to have stable flow characteristics, better performance and higher efficiency. The differences in the characteristics of old and modern ones cannot be explained solely by systematic error resulting from the difference in the accuracy of the instruments. This change in pump characteristics applies not only to their main area of operation i.e. positive flow, head, torque and speed but also to other areas in which the pump can, for example, operate with negative flow, head or torque. Knowing the characteristics in just such areas is needed, for example, to simulate failures in pumping systems because then the pump can operate with negative flows. Using publicly available older characteristics can lead to errors.

The complete characteristics of the pump including all possible modes of operation are presented in the graph *n* – speed as the independent variable and *Q* – flow rate as the dependent variable (Figure 1). Four basic parameters of pump operation are outlined, i.e. head *H*, flow rate *Q*, torque *M* and speed *n*. In a typical pumping mode, all of these parameters (*H, Q, M, n*) are positive, but in some other modes the rotodynamic pump operates with one or more of these parameters being negative. Since each of these four parameters can be positive or negative, the number of combinations is 16. However, 8 basic combinations or modes of operation are considered. Four of these eight modes are useful and can be used to convert energy – from mechanical in the shaft to hydraulic in the fluid or vice versa: there is a normal pumping mode at positive speed ($H > 0$, $Q > 0$, $M > 0$, $n > 0$ – area A) or negative speed ($H > 0$, $Q > 0$, $M > 0$, $n < 0$ – area E) and a turbine mode ($H > 0, Q < 0, M > 0, n < 0$ – area C) or reverse turbine mode ($H < 0, Q > 0, M < 0, n > 0$ – area G). Four modes are usually undesirable, due to energy dissipation.

A complete characteristic of the pump in all eight modes is required to determine the pump's operation in case of failure, startup, shutdown or non-standard conditions such as *PAT*.

Figure 1 shows the possible areas of operation in *n* and *Q* coordinates.

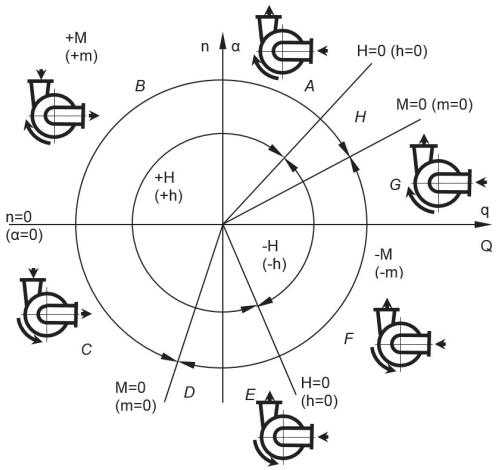

Figure 1 Possible areas of operation of the rotodynamic pump

The dimensionless values of the parameters are determined according to:

$$q = \frac{Q}{Q_n}; \quad h = \frac{H}{H_n}; \quad m = \frac{M}{M_n}; \quad \alpha = \frac{n}{n_n} \tag{1}$$

The representation of the pump characteristics in the form of a bunch of curves is inconvenient for further analysis, so the form of homologous curves appeared.

$$\frac{h}{\alpha^2} = f\left(\frac{q}{\alpha}\right) \; or \; \frac{h}{q^2} = f\left(\frac{\alpha}{q}\right) \tag{2}$$

$$\frac{m}{\alpha^2} = f\left(\frac{q}{\alpha}\right) \; or \; \frac{m}{q^2} = f\left(\frac{\alpha}{q}\right) \tag{3}$$

In 1966, Suter proposed a more convenient form (Equations (4)…(6)).

$$\tan(\theta) = \frac{q}{\alpha} \tag{4}$$

$$WH = \frac{h}{q^2 + \alpha^2} = f_1(\theta) \tag{5}$$

$$WM = \frac{m}{q^2 + \alpha^2} = f_2(\theta) \tag{6}$$

Pump manufacturers generally measure and provide pump characteristics in operation area A that is, for positive parameters (*H, Q, M, n*) and in other

areas (B, D, C, E, F, G, H) they do not do such tests. This is because of the cost and limited needs of the average pump user. Hence, studies of complete pump characteristics are usually performed by independent research teams. Such studies are scarce. Few older studies from more than half a century ago and few modern ones are available.

The measurement results obtained by many authors create a cloud of points, which for simulation must be approximated in the form of a function.

There is no universal function used for all specific speeds encountered, due to the small number of data as well as the very high complication if such a function was created. Therefore, function is defined for the measurement data corresponding to a particular pump.

The $WH(\theta)$ and $WM(\theta)$ values can be approximated in many ways. If these are polynomials, due to the difficulty of such an approximation in the entire range $0 \leq \theta \leq 2\pi$, they are usually defined in several sub-ranges, which requires the use of several functions. In this work, the experimental results were approximated using harmonic functions. This type of approximation has advantage over polynomial approach because $WH(\theta)$ and $WM(\theta)$ can be described by only one function.

The third-order harmonics were selected as giving the best accuracy in relation to the order. It was found that harmonics of higher orders do not offer significantly better accuracy remarkably expanding the function.

The failure of the feed pump was simulated, and the results were compared for older data, for our own data and for approximations by third-degree harmonic functions.

2 A Review of Existing Studies

The first step to identify abnormal modes of operation began in the 1930s with research by C.P. Kittredge and D. Thoma [3] for a low-speed centrifugal pump. The study, as the authors point out, did not allow precise determination of all parameters, but gave a picture of the pump's operation when they changed from negative to positive.

In 1937, in a publication [4], R.T. Knapp summarized earlier partial studies conducted at the Pasadena Institute and presented complete characteristics of a commercial pump with specific speed of 33, W.M. Swanson [5] in his work examined 16 years later the complete characteristics ($0 \leq \theta \leq 2\pi$ i.e. a range from A to H) for a radial flow, mixed flow and axial flow pump with specific speeds of 35, 147, 262, respectively. These characteristics are quite well known and were, among others, presented at A.J. Stepanoff [6] and in

the form of tables at E.B. Wylie, V.L. Streeter [7]. In further analyses, data from this book were used for comparisons.

In 1980 R. J. Brown, D. C. Rogers published [8] the results of field tests for four pumps with specific speeds of 15.7, 25.6, 28.9, 30.3 in the range of $1/8\pi \leq \theta \leq 8/5\pi$ i.e. from B to part of G. These tests were carried out under conditions of simulated pump failure (power loss) and due to the difficulty of measuring instantaneous flow, the values were calculated by software. They presented their results as well as those of previous authors in the form of tabulated Suter functions. In 2005, I.A. Lipatov et al. [9] investigated the full 4-quart characteristics of a pump with a specific speed of 11. The model pump was tested in the original full-scale circuit. The measurement area covered all modes from A to H. Data were presented in homologous form according to Equations (2) and (3) An extensive study was presented in 2009 in a paper [10]. The authors conducted tests on six pumps with specific speeds 20, 23, 33, 55, 105, 209, 261. The results were presented in the form of Suter curves in the full range of pump operation $0 \leq \theta \leq 2\pi$ and compared with older studies.

In 2012, in an article [11], I. S. Yoo et al. investigated a mixed-flow pump with reference diameter $d_2 = 368.2$ mm, and specific speed of 75.4, power of 135 kW and nominal flow of 2000 m^3/h with a vertical shaft. The pump was a model of a nuclear reactor cooling pump. Data were presented in homologous form according to Equations (2) and (3) and covered full range of pump operation from A to H. In 2017, in a paper [12], R. Zhu et al. presented the homology curves of a nuclear reactor cooling pump with specific speed of 96. The pump worked in the full range of operation (A to H).

In a 2018 paper [13], K. Karaskiewicz presented brakedown simulation for two modern centrifugal pumps with specific speeds $n_q = 16$ and 20 and compared them with the characteristics of old pumps presented in [4], showing that the differences in characteristics affect the dynamics of the pumping system.

The following papers describe the case of pump operation in PAT mode (Area C).

In 2005 in P.H.D. [14] P. Singh studied pumps with specific speeds of 24.5, 35.3, 36.4, 39.7, 45.2, 46.4, 79.1 and 94.4. The author presented characteristics of the head coefficient and efficiency from the flow coefficient $\psi(\varphi), \eta(\varphi)$.

In 2008 S. Derakhshan, A. Nourbakhsh presented in [15] the results of a study for a pump with a specific speed of 23.5. They calculated ψ, φ, π, η in *BEP* and compared with theory. In 2013, in an article [16] by A. Couzinet at

al. the study of a single-stage pump of the specific speed of 70 was presented. Unfortunately, there is no scheme (although there is a simple description) of the test bed. In 2016 In the article [17] X. Tan, A. Engeda investigated and compared with theoretical calculations the characteristics of 4 pumps with specific speeds 28.19, 28.17, 52 and 65.3. In 2017 S. Barbarelli et al. in [18] presented results for a range of pumps with specific speeds of 9.08, 9.43, 12.82, 16.34, 20.23, 25.43, 28.72, 30.31, 34.11, 43.48, 53.01, 64.07.

Measurements restricted to the PAT area are not sufficient to analyze the pump operation in failure conditions.

3 Test Bed Description

Section 3 presents the layout and simplified diagram of the test stand with basic measurement devices and presents the range of operating parameters obtained there.

Figure 2 shows a schematic of the test bed. The main components of the bed are the tested (1) and feed (5) centrifugal pumps, driven by speed-controlled motors. The task of the feed pump is to create a pressure that allows the tested pump to operate with negative flow.

The pump under test operated at BEP with parameters: $Q = 83$ m^3/h, $H = 85$ m, $n = 2960$ rpm, $M = 96.1$ Nm, $P = 29.42$ kW.

Control valves (directly after pumps and collector) are used to regulate the output, which also act as shut-off valves in the various stages of testing. The remaining valves are shut-off valves, used to establish the subsequent operating areas (A), (B), (C),..., of the pump (1).

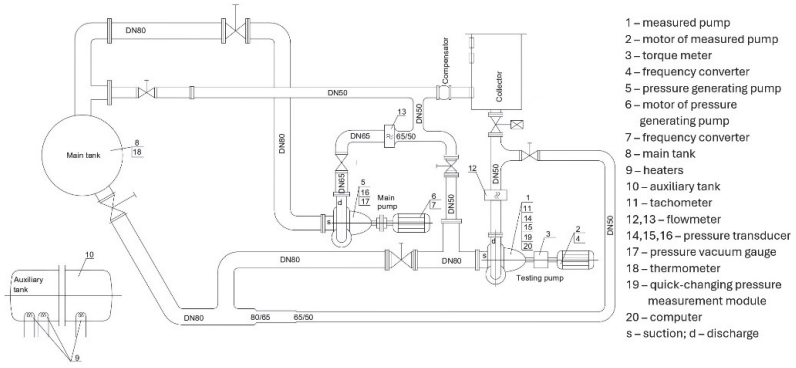

Figure 2 Functional diagram of the test bed; individual components of the test bed are described in the text.

The vertical tank (8) with a capacity of about 12 m^3 has a triple role:

– it is an equalization tank
– provides an inflow height of $H_z = 1.5...5.0$ m, depending on the need
– due to its large thermal capacity, allows the water temperature to remain constant during testing.

During turbine operation, the asynchronous motor operated as a generator, transmitting turbine power via a brake-chopper inverter to the load. In both cases, the power consumer was a set of three heaters of 13.5 kW each (17) placed in a large horizontal tank (18) $V = 8$ m^3. In the case of the 3-phase motor/generator, each heater was connected to a different phase. The large thermal capacity of the tank made it possible to run the pump in turbine motion for long periods of time without the risk of overheating the water.

4 Accuracy Discussion of WH and WM Measurement

Section 4 presents the calculation method and the measurement uncertainty values obtained at this test stand.

Measurements of the $n_q = 16$ pump were carried out in laboratory stage. To measure all needed parameters, the following devices were used:

a. differential manometer class 0.1, range 40 bar displaying two decimals,
b. flowmeter class 0.25, range 100 m^3/h displaying decimals,
c. torque meter class 0.1, range 150 Nm displaying two decimals,
d. rotational speed set circuit displaying two decimals

To determine the measurement uncertainty of $WH(\theta)$ and $WM(\theta)$ curves the method of complete differential was used with the following formula (according to [19]):

$$u_{WH}(h,q,\alpha) = \sqrt{\left(\frac{\partial(WH)}{\partial h}\cdot u_h\right)^2 + \left(\frac{\partial(WH)}{\partial q}\cdot u_q\right)^2 + \left(\frac{\partial(WH)}{\partial \alpha}\cdot u_\alpha\right)^2} \quad (7)$$

$$u_{WM}(m,q,\alpha) = \sqrt{\left(\frac{\partial(WM)}{\partial m}\cdot u_m\right)^2 + \left(\frac{\partial(WM)}{\partial q}\cdot u_q\right)^2 + \left(\frac{\partial(WM)}{\partial \alpha}\cdot u_\alpha\right)^2} \quad (8)$$

$$u_\theta(q,\alpha) = \sqrt{\left(\frac{\partial\theta}{\partial q}\cdot u_q\right)^2 + \left(\frac{\partial\theta}{\partial \alpha}\cdot u_\alpha\right)^2} \quad (9)$$

where: u_h, u_q, u_α is the measurement uncertainty of *h*, *q* and α.

Given the pump specification ($Q_n = 81.7$ m^3/h, $H_n = 86$ m, $M_n = 96$ Nm, $n_n = 2923$ rev^{-1}) and specifications of the measurement devices, u_h, u_q, u_α($u_h = 0.001$; $u_q = 0.00289$; $u_m = 0.005$; $u_\alpha = 0.00001$), and u_{WH} and u_{WM} were calculated. The values of u_{WH}, u_{WM} and u_α were calculated for Best Efficiency Point and as following: $u_{WH} = 0.00187$ m, $u_{WM} = 0.0031$ Nm, $u_\alpha = 0.00144$ rad.

5 Mathematical Analysis

Section 5 presents the method of mathematical description of measurement results used in the article, a summary of the obtained measurement results, and a short discussion of the validity of this method of description.

The basic field of *WH*(θ) and *WM*(θ) has the range $0 \div 2\pi$ and can be treated as a periodic function, because the values at the ends of this range are the same. These curves for pumps of only one specific speed value could be described by a function of a simple form, however, as previously presented, such curves have different shapes and finding one function which would be convenient to use and which would describe them well is not a simple task. The approximation of these curves by means of polynomials or, for example, spline functions requires using polynomial of degree 10. However, thanks to their periodic character, it is possible to choose the distribution of functions into a Fourier series for this analysis:

$$f(\theta) = \frac{1}{2}a_0 + \sum_{n=1}^{\infty}[a_n cos(n\theta) + b_n sin(n\theta)] \tag{10}$$

Where $f(\theta)$ denotes *WH*(θ) or *WM*(θ), and coefficients a_0, a_n i b_n can be calculated using the following formulae:

$$\left.\begin{aligned} a_0 &= \frac{1}{\pi}\int_0^{2\pi} f(\theta)d\theta \\ a_n &= \frac{1}{\pi}\int_0^{2\pi} [f(\theta)cos(n\theta)]d\theta \\ b_n &= \frac{1}{\pi}\int_0^{2\pi} [f(\theta)sin(n\theta)]d\theta \end{aligned}\right\} \tag{11}$$

To use formula (10) and to find coefficients (11), numerical integration using small $\Delta\theta$ step was done with an angle θ varying in the range $0 \div 2\pi$. The third-order Fourier decomposition coefficients are shown in Table 1, and their absolute values are shown in Figures 3 and 4.

Table 1 Coefficients of Fourier transformation for a pump of $n_q = 16$

	a_0	a_1	b_1	a_2	b_2	a_3	b_3
WH	0,856	−0,306	0,410	0,466	0,103	0,087	−0,028
WM	0,138	−0,477	0,336	−0,067	0,302	0,086	−0,021

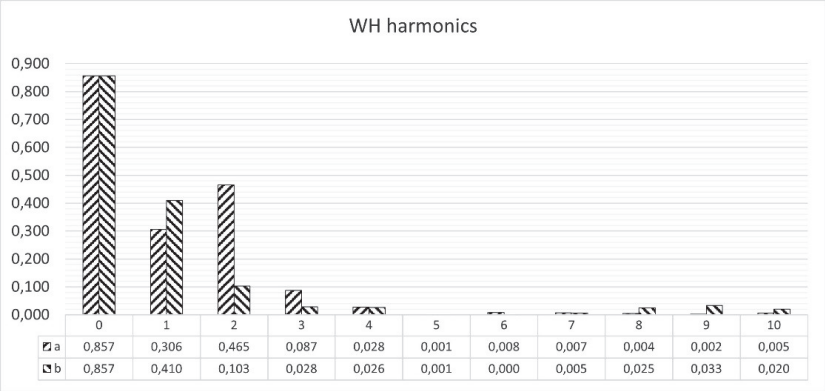

Figure 3 Absolute values of harmonic coefficients for *WH*.

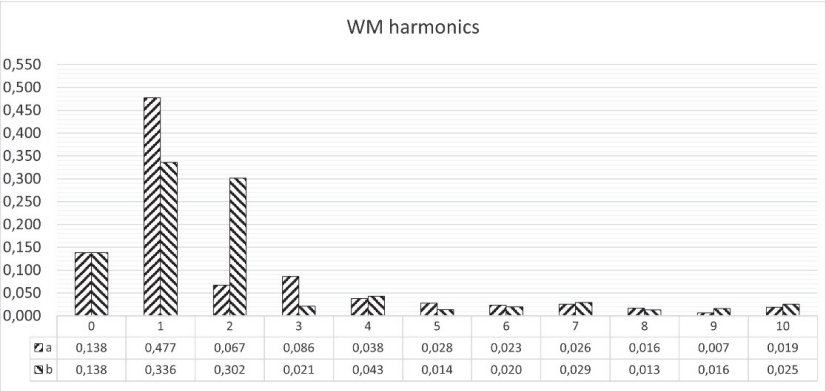

Figure 4 Absolute values of harmonic coefficients for *WM*.

Figures 5 show the values of *WH* and *WM* coefficients in the whole range of θ angle, i.e. from 0 to 2π. In the same figures, for comparison, values *WH*_F and *WM*_F interpolated by trigonometric functions are shown.

The Fourier approximation of various orders was checked. It turned out that the third-order approximation was accurate enough, and this one was accepted for further analysis.

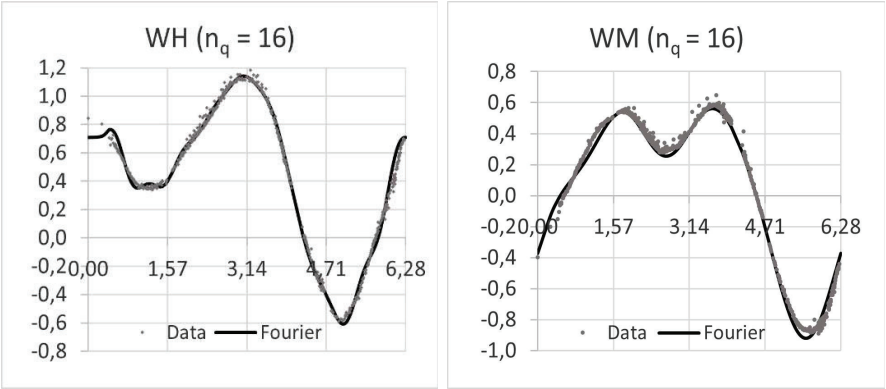

Figure 5 *WH* and *WM* curves for specific speed n_q = 16 pump for the third order Fourier approximation.

6 Checking the Fitting by Sensitivity Analysis

Section 6 presents a short description of the real physical system, where the matching of the obtained mathematical description to the real case was checked through sensitivity analysis. It is also a preliminary description for the next two sections.

Suter curve describes the centrifugal pump behavior in four quadrants, therefore the influence of the Suter curve fitting on the pump system dynamics can be checked by sensitivity of the system against the fitting.

The feedwater system of a typical 200 MW unit was analyzed (Figure 6). Sensitivity analysis was carried out for such a unit. Details are given in [13]. For comparison with experimental data of a modern pump with specific speed $n_q = 16$ Fourier fitting was used as well as the experimental data from V.L. Streeter's and E.B. Wylie work [6] for an older type pump from over a half century ago.

The pump's breakdown due to a power failure was simulated and its operation in the first second was analyzed.

7 Basic Dynamic Equations and Numerical Model

This section shows the mathematical model used in the described real case of pump operation in a high inertia water circuit and dynamically changing hydraulic parameters. It also shows a comparison of this model to a model obtained using a Fourier series.

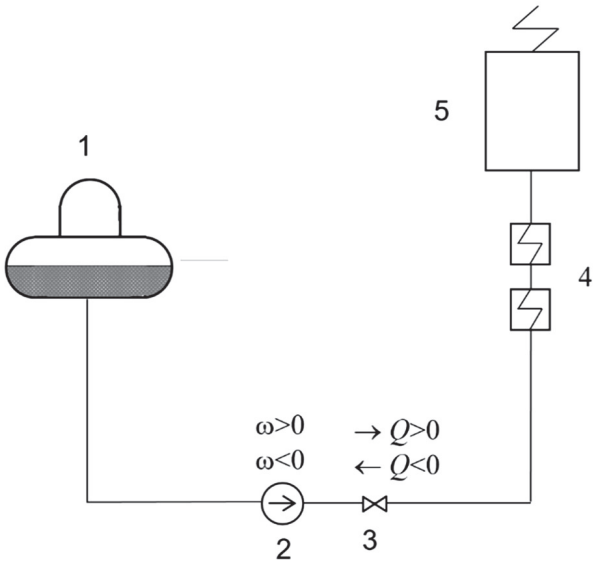

Figure 6 Feed water pumping system.

The following set of dynamics equations for translational and rotational motion was solved:

$$H(Q,\omega) = H_{stat} + aQ|Q| + \frac{l}{gA}\frac{dQ}{dt} \tag{12}$$

$$M_s(Q,\omega) = I\frac{d\omega}{dt} + M_t + M_p \tag{13}$$

where:

M_s – motor torque,
M_t – the sum of friction moments in the gland and the bearings of the pump and motor,
M_p – the moment passing to the liquid through the impeller of the pump (hydraulic torque);

Initial conditions for the pump are set by the nominal parameters: $Q(0) = Q_n$, $\omega(0) = \omega_n$, $H(0) = H_n$, $M_p(0) = M_n$ and for the motor by: $M_s = 0$.

Characteristics of $WH(\theta)$ and $WM(\theta)$ for breakdown simulation cover the values of θ between 2 and 4 and are shown in Figure 7. Fourier fitting and experimental data curves are very close to each other for *WH* coefficient and *WM* coefficient but there is some discrepancy between both and Streeters

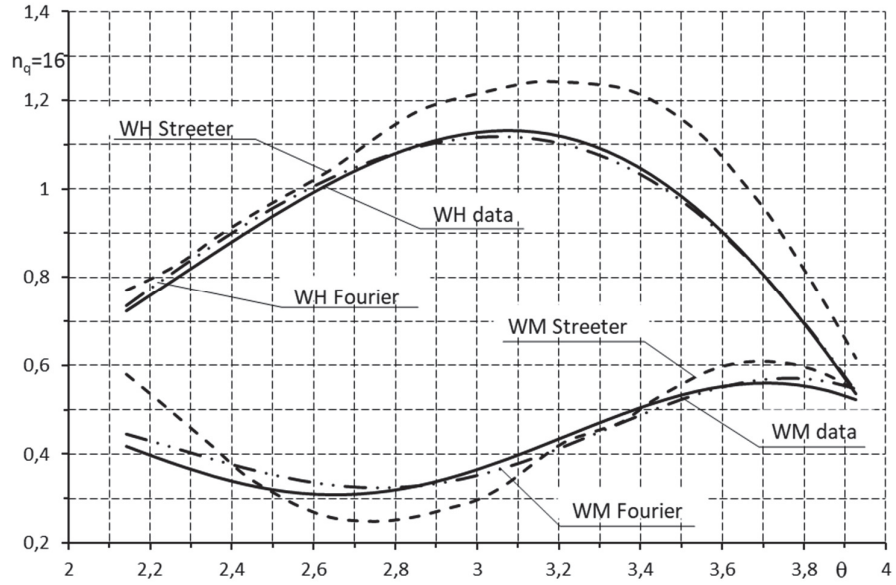

Figure 7 *WH* and *WM* characteristics in the region of pump operation.

data curve. This shows that over the last few decades the characteristics of pumps have changed and that using old ones for simulation in the absence of experimental data for new ones can imply large discrepancies.

8 Discussion of Breakdown Simulation Results

Section 8 presents a comparison of the time variability of the parameters obtained in the simulation described by the model in Section 7 with the parameters obtained using the Fourier series described in Section 5.

The variations in flow and angular velocity are shown on Figure 8. The results based on the Fourier fitting coincide with the results based on the experimental data, whereas the results for the Streeter data differ, which results from the differences in Suter characteristics for these cases.

The flow and angular velocity in the latter case decrease faster. Figure 9 shows variations in the head of torque. There is a change in flow between 0.2 sec and 0.3 sec from positive to negative, which implies head and torque changes with a minimum value in this range. Again, the Fourier fitting curve and the experimental curve is different from the Streeter curve, which is directly caused by the differences in flow and angular velocity variations.

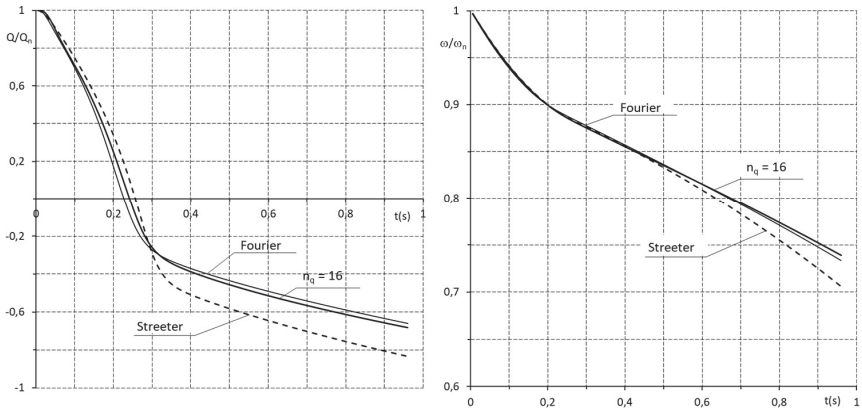

Figure 8 Variation of flow rate and rotational speed of the pump during breakdown.

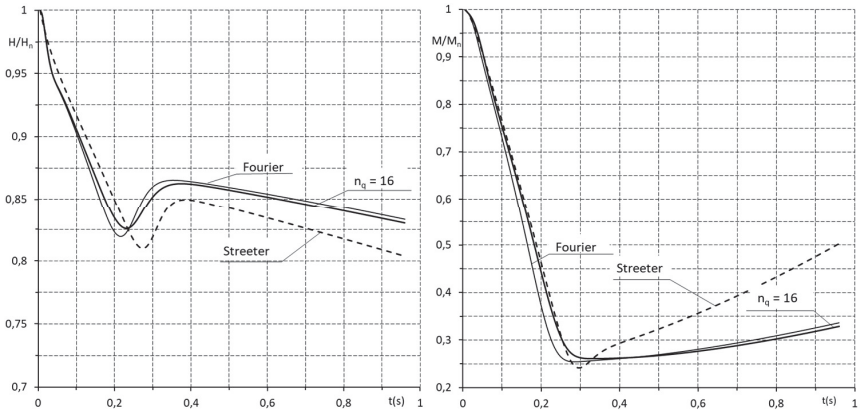

Figure 9 Variation of head and torque the pump during break down.

From the simulation graphs, it can be seen that Fourier fitting curve almost coincides with the curve of experimental data and can be a convenient substitute for raw measurement data.

9 Conclusions

1. The experimentally obtained values *WH* and *WM* were approximated by third-order harmonics, since higher harmonics increased the accuracy of the approximation very little decreasing simplicity of the final function.

A good fit to the experimental data was obtained for the whole range of pump operation in all pump modes.
2. Unlike approximation using e.g. polynomials, the use of harmonics allows for high accuracy using one function.
3. It was decided to check to what extent differences in the characteristics of a pump with the same specific speed affect the dynamics of the system during failure. A simulation of a feed water pump failure in the system of a 200 MW unit was performed. Three different characteristics of the feed pump were used for the simulation. The first characteristic was based on studies of a pump from half a century ago. The second characteristic was based on studies of a contemporary pump. The third characteristic was based on the approximation of the measurement data of the contemporary pump with a third-order harmonic.
4. The simulation results show that the difference between the old characteristics and the modern characteristics significantly affects the changes in parameters such as head, flow, torque and speed over time.
5. The analysis carried out in this paper suggests that when analyzing the failure of a contemporary pump, if possible, it is better to use characteristics obtained contemporarily.

Funding

This study was a funded by the Ministry of Science and Higher Education Republic of Poland (MNiSW) (No nr N N513 331038).

Conflicts of Interest

The authors declare no conflict of interest.

References

[1] A. Papierski, A. Błaszczyk, Multilevel Optimization of the Semi-Open Impeller in a Centrifugal Pump, Mechanics and Mechanical Engineering, Vol. 15, No. 3 (2011) 319–332.

[2] H. Ayremlouzadeh, S. Jafarmadar, S. Reza, A. Niaki, 'Investigation on the Effect of Impeller Design Parameters on Performance of a Low Specific Speed Centrifugal Pump Using Taguchi Optimization Method', International Journal of Fluid Power, vol. 23 Iss 2, pp. 161–182. doi: 10.13052/ijfp1439-9776.2322.

[3] D. Thoma, 'Vorgäange beim Ausfallen des Antriebes von Kreiselpumpen', Mitteilungen des Hydralischen Instituts der Technischen Hochschule München, vol. 4, pp. 102-104; also Kittredge, C.P., Thoma, D., 1931, "Centrifugal Pumps Operated Under Abnormal Conditions", Power, June 2, pp. 881–884, 1931.
[4] R. T. Knapp, 'Complete Characteristics of Centrifugal Pumps and Their Use in Prediction of Transient Behavior', Trans. ASME, vol. 59, pp. 683–689, 1953.
[5] W. M. Swanson, 'Complete Characteristic Circle Diagrams for Turbomachinery', Trans. ASME Journal of Fluids Engineering, 75(5), pp. 819–826, 1953.
[6] A. J. Stepanoff, 'Centrifugal and Axial Flow Pumps', J.Wiley: N.York, USA, 1957.
[7] E. B. Wylie, V. L. Streeter, "Fluid Transients in Systems', Journal of Fluid Mechanics, Vol. 264, 1993. DOI: https://doi.org/10.1017/S00221 12094210716.
[8] R. J. Brown, D. C. Rogers, 'Development of Pump Characteristics from Field Tests', Journal of Mechanical Design, ASME, 102(4), 1980. DOI: 10.1115/1.3254826.
[9] I. A. Lipatov, I. V. Elkin, A. I. Antonova, G. I. Dremin, A. V. Kapustin, S. M. Nikonov, A. A. Rovnov, V. I. Gudkov, 'Four-quadrant characteristics of PSB-VVER pumps'. Proceedings of the International Conference Nuclear Energy for New Europe 2005, Bled, Slovenia, September 5–8, 2005, pp. 056.1–10, 2005.
[10] E. Ayder, A. N. Ilikan, M. Sen, C. Özgür, L. Kavurmacioğlu, K. Kirkkopru, 'Experimental investigation of the complete characteristics of rotodynamic pumps', ASME 2009 Fluids Engineering Division Summer Meeting, Vail, Colorado, 2–6 August, pp. 35-40, 2009.
[11] I. S. Yoo, M. R. Park, S. C. Hwang, E. S. Yoon, 'Complete Characteristic Curve for a Reactor Coolant Pump', Journal of Fluid Machinery, Vol. 15, no. 5, 2012.
[12] R. Zhu, Y. Liu, X. Wang, Q. Fu, A. Yang, Y. Long, 'The research on AP1000 nuclear main pumps' complete characteristics and the normalization method'. Annals of Nuclear Energy, 99, pp. 1–8, 2017.
[13] K. Karaśkiewicz, 'Sensitivity analysis for power plant pumping systems in breakdown', Archive of Mechanical Engineering, 65, pp. 349–359, 2018.

[14] P. Singh, 'Optimization of Internal Hydraulics and of System Design for pumps as turbines with field implementation and evaluation', PhD dissertation, Universität Fridericiana zu Karlsruhe, 2005.
[15] S. Derakhshan, A. Nourbakhsh, 'Theoretical, Numerical and Experimental Investigation of Centrifugal Pumps in Reverse Operation', Experimental Thermal and Fluid Science, 32, pp. 1620–1627, 2008.
[16] A. L. Couzinet, L. Gros, D. Pierrat, 'Characteristics of Centrifugal Pumps Working in Direct or Reverse Mode: Focus on the Unsteady Radial Thrust', International Journal of Rotating Machinery, 2013. DOI: 10.1155/2013/279049.
[17] X. Tan, A. Engeda, 'Performance of Centrifugal Pumps Running in Reverse as Turbine Part II Systematic Specific Speed and Specific', Renewable Energy, 99, pp. 188–197, 2016.
[18] S. Barbarelli, M. Amelio, G. Florio, 'Experimental activity at test rig validating correlations to select pumps running as turbines in microhydro plants', Energy Conversion and Management, 149, pp. 781–797, 2017.
[19] Joint Committee for Guides in Metrology, 'Evaluation of measurement data – Guide to the expression of uncertainty in measurement', 2008.

Biographies

Krzysztof Karaśkiewicz received the master's degree in Mechanical Engineering from Warsaw University of Technology in 1979, and the philosophy of doctorate degree in Mechanical Engineering from Warsaw University of Technology in 1994. He worked in the pumping industry running the research and development department, among other things. He is currently working as an Associate Professor at the Department of Rational Use of Energy, Faculty of Power and Aeronautical Engineering, Warsaw University of Technology.

His research areas include pumps, pumping systems, fluid transients, energy efficiency in power engineering and in the industry.
https://orcid.org/0000-0003-4709-2355.

Jacek Szymczyk was born in Warsaw, Poland, in 1975. He received his master's degree in Mechanical Engineering from Warsaw University of Technology in 2001, and the philosophy of doctorate degree in Mechanical Engineering from Warsaw University of Technology in 2007. He is currently working as an Assistant Professor at the Department of Rational Use of Energy, Faculty of Power and Aeronautical Engineering, Warsaw University of Technology. His research areas include pumps and pumping systems, industrial water purification, energy storage and harvesting, and energy efficiency in power engineering and in the industry.
https://orcid.org/0000-0002-9718-6467